

Global-scale patterns of observed sea surface salinity intensified since the 1870s

W. John Gould ¹✉ & Stuart A. Cunningham ²

Sea surface salinity patterns have intensified between the mid-20th century and present day, with saline areas becoming saltier and fresher areas fresher. This change has been linked to a human-induced strengthening of the global hydrological cycle as global mean surface temperatures rose. Here we analyse salinity observations from the round-the-world voyages of *HMS Challenger* and *SMS Gazelle* in the 1870s, early in the industrial era, to reconstruct surface salinity changes since that decade. We find that the amplification of the salinity change pattern between the 1870s and the 1950s was at a rate that was $54 \pm 10\%$ lower than the post-1950s rate. The acceleration in salinity pattern amplification over almost 150 years implies that the hydrological cycle would have similarly accelerated over this period.

¹National Oceanography Centre European Way, Southampton, UK. ²Scottish Association for Marine Science, Scottish Marine Institute, Oban, Argyll, UK.
✉email: wjg@noc.ac.uk

The scientific definition of salinity started in the 1890s and only in the Atlantic¹ has it been possible to document salinity changes into the 19th century. For the voyages of *HMS Challenger* (1872–1876)² and *SMS Gazelle* (1874–1876)³, which took place early in the industrial era⁴, we have derived absolute salinity⁵ from the specific gravity measurements at the almost 400 stations occupied (Fig. 1a). The process of converting specific gravity observations to salinity and the assessment of the data quality are described in the “Methods” section. When combined with 20th century reconstructions of the global salinity field, the data allow us to assess changes in surface salinity globally over almost 150 years.

We focus the analysis on three periods, the 1870s and the decades centred on 1954 and 2014. This allows comparisons with other analyses describing salinity change between the latter two periods^{6–9}. The 1870s data are compared with the 5 m salinity values in the EN4 (Version 4.2.1)¹⁰ data set. We chose the EN4 data set because it is based solely on observational data. We also repeated the analysis using the newer Cheng et al.⁹ data set, which relies on CMIP5¹¹ output.

Results and discussion

Patterns of salinity change since the 1870s. We noted that the regional patterns of change between the 1950s and 2008 reported by⁷ showed saline areas becoming more saline and the fresh areas

fresh, an amplification (defined as the amplitude of the change between saline and fresh regions) believed to be indicative of strengthening of the global hydrological cycle since the mid-20th century and summarised in^{7,8}.

In order to reveal whether the patterns of change between the 1870s and the 1950s might have been similar to those since the 1950s we identified regional groups of *Challenger* and *Gazelle* stations, the positions of which lay in distinct areas of post-1950s freshening or salinification revealed by the EN4 5 m fields representing the salinity difference from the decadal averages, 1950 to 1959 and 2010 to 2019.

Figure 1a shows the *Challenger* and *Gazelle* station positions in relation to the mean EN4 5 m surface salinity field (1950–2019). The regionally- grouped 1870s stations are shown in Fig. 1b, *Challenger* and 1c *Gazelle*). The stations in each regional group are listed in Supplementary Table S1.

The areas traversed by *Challenger* and *Gazelle* were marked by salinification in the subtropical gyres of the North and South Atlantic and South Indian Oceans (*Gazelle* only). Freshening is seen in the low-latitude western Pacific, the equatorial Atlantic and the Southern Ocean. The patterns of change from the EN4 data are similar to those reported by^{6–8} between the 1950s and 2012.

For each of these station groups we computed mean rates of salinity change from the 1870s to the mean decadal average EN4

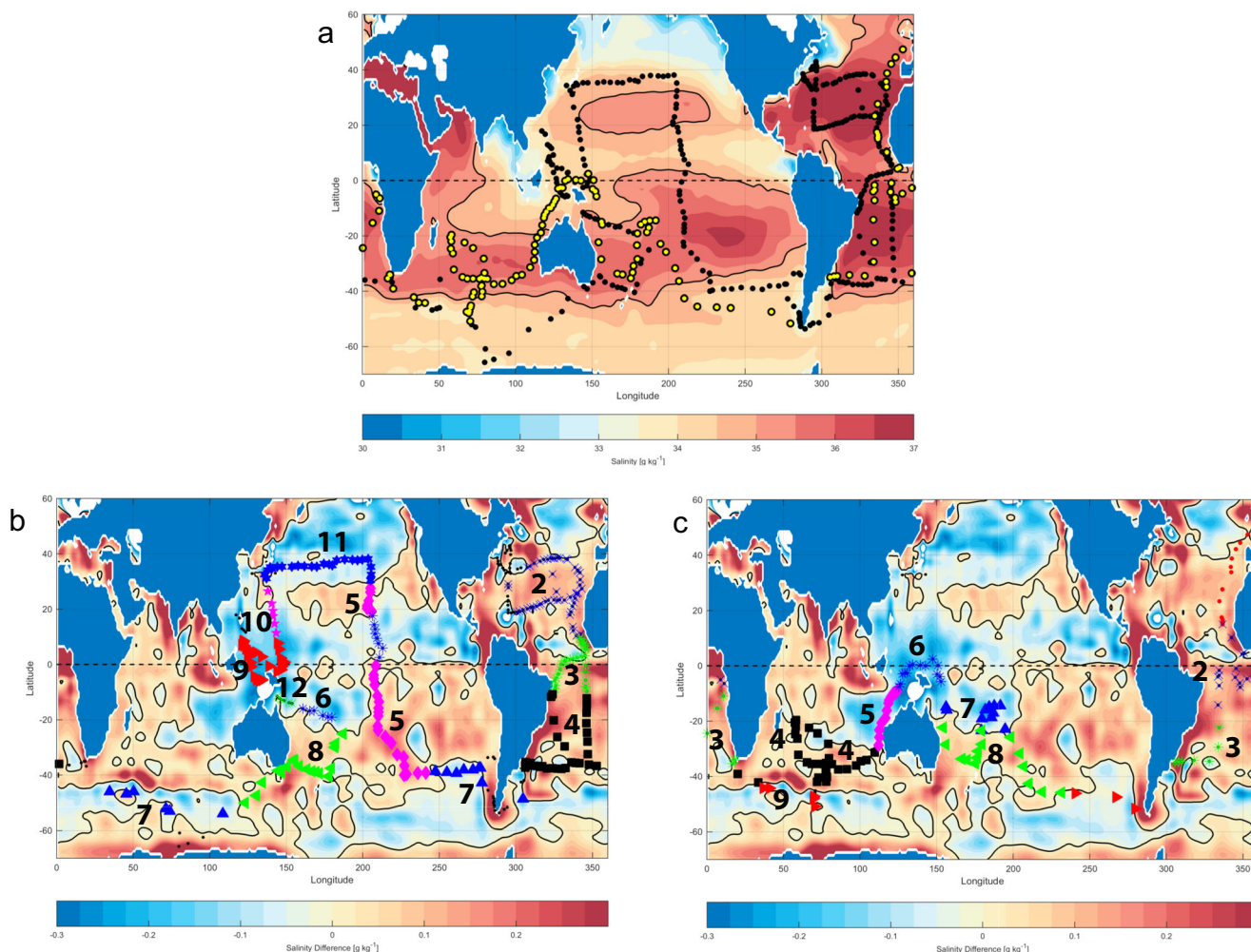


Fig. 1 Challenger and Gazelle stations in relation to recent salinity fields. **a** Challenger (black) and Gazelle (yellow) station positions superimposed on the mean (1950–2019) EN4 5 m salinity field. Bold line is 35 g kg⁻¹ contour. **b** (Challenger) and **c** (Gazelle) stations with regional groupings overlaid on EN4 5 m salinity change (2010–2019 minus 1950–1959). Station groupings key and definition of areas are given in Fig. 2 and Table S1.

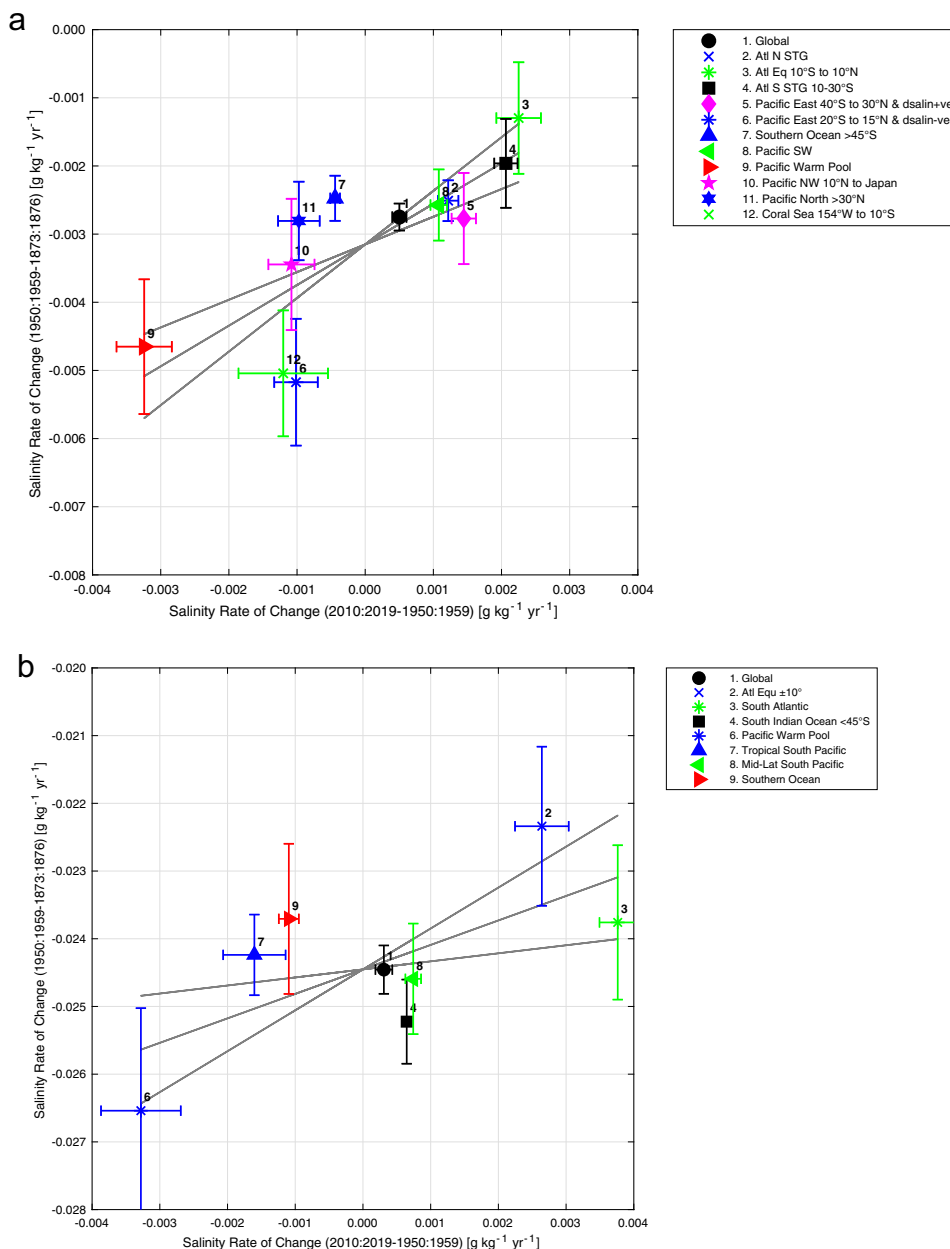


Fig. 2 Regional salinity changes from the 1870s to the 1950s and from the 1950s to the 2010s. a Rates of salinity change (per annum) of Challenger and **b** Gazelle data (EN4(1950–1959) minus 1870s) versus (EN4(2010–2019) minus EN4(1950–1959)). Each is scaled by the time span (1873 to 1954, 81 years), (1955 to 2015, 60 years). The error bars for the 1870s reflect the variations within each region. For EN4 the error bar is ± 1 standard deviation of monthly mean 5 m value and the total error in ordinate or abscissa is computed as the root-sum-square error from each component. The least-squares fit and 95% confidence limit is given by the black lines. The degrees-of-freedom to estimate the fit is the total number of samples divided by the number of regions (for Challenger dof = 24; for Gazelle dof = 13).

5 m salinity (1950–59) and compared these with the changes from the 1950s to 2010–19. These comparisons are in Fig. 2.

The plots show a stronger correlation for *Challenger* than for *Gazelle*. This reflects the wider regional distribution and larger number of *Challenger* stations (285 after 15 rejected) than *Gazelle* (101 after 9 rejected) stations in the regional analysis. The areas of strongest and most consistent change since the 1870s are freshening of the Pacific Warm Pool (*Challenger* and *Gazelle*) and salinification in the North and South Atlantic subtropical gyres (*Challenger*) and equatorial Atlantic (*Gazelle*).

The ratio of the regional salinity rate of change in these two periods is a measure of the salinity amplification. For the *Challenger* data there is a clear linear relationship between the

rates of change (slope 0.6 ± 0.2 , correlation coefficient 0.64). The equivalent figures for *Gazelle* are, slope 0.4 ± 0.3 , correlation coefficient 0.36. The slopes are statistically inseparable. We also computed the equivalent relationships using the Cheng (CZ16) data set for which the corresponding slopes and correlation coefficients were *Challenger* (0.51 ± 0.31 , 0.33) and *Gazelle* (0.66 ± 0.46 , 0.43).

In these analyses all regions were given equal statistical weight even though they contained differing numbers of stations. We chose this simple approach because the stations are not equally spaced and thus the number of stations cannot be seen as representative of the track length (area) in which changes occur.

To convert the rate of change in the salinity amplification to a salinity anomaly in the 1870s we first computed the global salinity change in the EN4 data sets between the decades centred on 1954 and 2014. (We excluded sea ice influenced areas north of 65°N from this analysis where EN4 salinities appeared anomalous and high latitude areas were not sampled in the 1870s). From EN4 we calculated the global mean salinity change in areas where salinity increased and in those where salinity decreased between 1955 and 2015. These values are respectively $+0.0940 \text{ g kg}^{-1}$ and $-0.0897 \text{ g kg}^{-1}$, giving a global amplitude of salinity amplification of 0.184 g kg^{-1} over 60 years. This implies that the rate of salinity amplification since 1955 is $0.306 \text{ g kg}^{-1} \text{ century}^{-1}$ (Table 1).

We then used the ratio of regional salinity changes, as represented by the slopes of Fig. 2, to project back to the 1870s. This calculation implies a mean salinity change between the 1870s and 1950s (based on analyses of *Challenger* and *Gazelle* and using EN4 and CZ16 data sets) of $0.133 \pm 0.041 \text{ g kg}^{-1}$, a rate of $0.166 \pm 0.052 \text{ g kg}^{-1} \text{ century}^{-1}$ (Table 1).

The ratio of pre-1950s rate of SSS change to post-1950s is $1:1.84 \pm 0.44$ (Table 1). Thus, we find that the rate of salinity pattern amplification before the 1950s was $54 \pm 10\%$ lower than the rate since the 1950s.

Implications for global hydrology. In order to investigate the insights that our estimates of salinity change might give into the global hydrological cycle we plot the salinity changes since the 1870s against changes in surface air temperature from the HadCRUT.5.0.1.0¹² data sets and sea surface temperature from HadSST.4.0.0.0¹³ in Fig. 3. These plots show that our salinity change results are consistent with the link described in⁶ between the rate of amplification, (fresh gets fresher - saline gets saltier) and temperature.

The statistics in Table 1 summarise the changes and rates of change of SST, SAT and SSS (from this study) plotted in Fig. 3 for the periods before and after the 1950s. While previous analyses of the relationship between salinity change and the global hydrological cycle have focussed on the relatively well-observed period since the 1950s during which changes in SAT and SST have been close to linear, this analysis includes the pre-1950s period which exhibited slower changes in SAT and SST. Figure 3 and the statistics in Table 1 suggest a closer relationship between SSS pattern amplification and SST changes than with changes in SAT over the 145 years of this study. The model-based analysis by Zika et al.¹⁴ of the post-1950s salinity pattern amplification (5–8%) attribute approximately half of that amplification to ocean surface warming (SST) with the remainder being linked to strengthening of the hydrological cycle.

Conclusions

The conversion of the *Challenger* and *Gazelle* specific gravity observations from the 1870s to equivalent absolute salinities produces values that are consistent with the large-scale surface salinity structure as defined by the EN4 data set. This holds good for the areas sampled by both expeditions covering all the major ocean basins. Furthermore, the salinity values are of high enough quality to permit meaningful estimates of the changes in salinity since the 1870s in areas of persistent freshening and salinification.

The 1870s data, being from a time-window before the rapid 20th century changes, allow us to study changes during a time span in which the rates of increase in both surface air temperature and sea surface temperature accelerated. The regional *Challenger* and *Gazelle* data when combined with the post-1950s EN4 and CZ16 products show that the pattern of salinity amplification (fresh areas becoming fresher, saline areas more salty) is consistent with the post-1950s pattern amplification reported by

Table 1 Summary of SST, SAT and SSS changes, 1870s to 1950s and 1950s to present.

Years	Time span years	SST change °C	SAT change °C	SST change rate °C century ⁻¹	SAT change rate °C century ⁻¹	SSS change g kg ⁻¹	SSS change rate g kg ⁻¹ century ⁻¹
(1870–79) to (1950–59)	80	0.170 ± 0.05	0.208 ± 0.055	0.213 ± 0.205	0.260 ± 0.068	CH/EN4 GZ/EN4	CH/EN4 GZ/EN4
				0.151 ± 0.024		CH/CZ16	CH/CZ16
				0.090 ± 0.043		GZ/CZ16	GZ/CZ16
				0.128 ± 0.039		Mean	Mean
				0.166 ± 0.058			
(1950–59) to (2010–19)	60	0.626 ± 0.05	0.822 ± 0.056	1.044 ± 0.091 (4.90)	1.370 ± 0.033 (5.27)	CH/EN4 GZ/EN4	CH/EN4 GZ/EN4
				0.184 ± 0.001		(GZ/EN4)	(1.63 ± 0.22)
						(CH/CZ16)	(2.71 ± 0.87)
						(GZ/CZ16)	(1.91 ± 0.45)
						Mean	(1.48 ± 0.38) (1.84 ± 0.44)

Changes and rates of change of Sea Surface Temperature (SST), Surface Air Temperature (SAT) and Sea Surface Salinity (SSS) over the periods 1870–1879 (and from 1873 for SSS) to 1950–59 and 1950s to 2010–19. The errors for SST and SSS are computed as the root-sum-square of the standard error (standard deviation divided by $\sqrt{10}$, assuming 10 annual values in decadal average are independent) for the decadal period in the published data. SSS error in the period 1950–2010 is a standard error measure of the mean positive and negative salinities. The SSS errors in the 1870s period are from the *Challenger* (CH) and *Gazelle* (GZ) analyses using the EN4 and CZ16 data sets. (Bracketed figures in lower row are the 1950s to present day rates divided by the 1870s to 1950s rates of change).

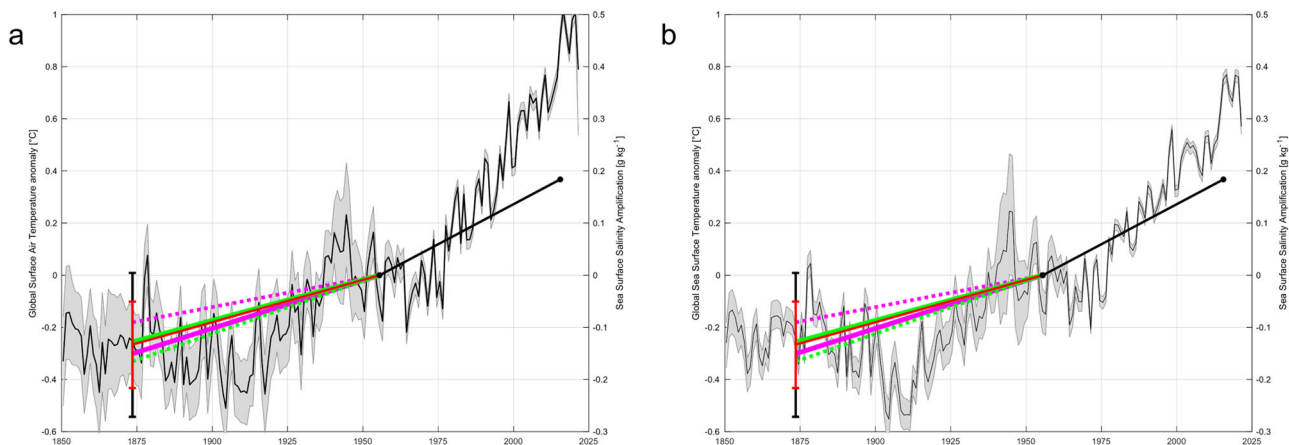


Fig. 3 Surface salinity changes since the 1870s compared with Surface Air Temperature (SAT) and Sea Surface Temperature (SST). Surface salinity (SSS) changes compared with changes in **a**, HadCRUT Surface Air Temperature (SAT) and **b**, HadSST Sea Surface Temperature (SST). Both data sets have been adjusted so that the average temperature anomaly for the period (1950–1959) is zero. The solid black line from 1954 to 2014 is the mean EN4 salinity change (2010–2019)–(1950–1959) between positive and negative salinity anomaly regions of 0.184 g kg^{-1} . The salinity change pre-1950s is determined from the comparison of the Challenger and Gazelle data to both EN4 and CZ16 data. The error bars are derived from the 95% confidence limits. Magenta solid CH(EN4), magenta dashed GZ(EN4), green solid CH(CZ16) and green dashed GZ(CZ16). The solid red is the mean of the slope and error from the four analyses.

Durack et al.⁸ in their investigation of the relationship of surface salinity changes to the global hydrological cycle. Our analysis shows that the pattern amplification has intensified with the value before the 1950s being $54 \pm 10\%$ lower than after that decade.

There are indications (Fig. 3) that this change in amplification over almost 150 years may be more closely aligned to changes in sea surface temperature than to changes in surface air temperature. The investigation of what light these data from the 1870s may shed on the interplay of SAT and SST in determining salinity pattern intensification¹⁴ is beyond the scope of this paper.

After the analysis of these two sparse and sub-optimally distributed data sets, the following quote by Hubble¹⁵ may be apposite. “For such scanty material, so poorly distributed, the results are fairly definite”.

Methods

Conversion of specific gravity to salinity. At the time of the expeditions there was no means of directly determining salinity but subsequently chemical analyses of Challenger data by Dittmar¹⁶ started the development of the concept of salinity based on the chlorinity of the samples¹⁷.

As noted earlier we converted the 1870s specific gravity measurements to equivalent absolute salinities. (We assumed that the specific gravity measurements corresponded directly to density, using the reference value of pure water at 0°C of 1.00 g cm^{-3}). The conversion of density to salinity used a modern-day equation of state (TEOS-2010)⁵ using the temperatures to which the 1870s data were standardised (15.56°C for the Challenger data and 14°Réaumur (17.5°C) for Gazelle).

The means of measuring specific gravity on Challenger are well documented. The narrative of the voyage¹ states that “Water from the surface was collected in the ordinary way in a bucket”. The Challenger reports also describe the determination of specific gravity and the subsequent conversion to a value at a standard temperature of 60°F . The ambient temperature was determined by a Geissler thermometer, the calibration of which was frequently checked in melting ice. Specific gravity determinations were made using a Buchanan hydrometer^{18–20} to which a series of standard weights could be added to accommodate a wide range of values while retaining a high sensitivity. The same hydrometer and weights were used throughout the voyage. Surface samples were drawn from a bucket and analysed immediately. The determinations of specific gravity were made on a swinging table to minimise the effects of ship motion and in rough weather measurements were delayed until calmer conditions prevailed. Every single measurement was made by the expedition’s chemist, J.Y. Buchanan, who noted that he locked the laboratory door to avoid distractions²¹, (page 24).

There is less information about the collection of the surface samples by Gazelle. The report states “S.M.S. “Gazelle” carried two different types of areometers for the scientific observations, model STEEGER-KÜCHLER and model GREINER. The STEEGER-KÜCHLER areometers were equipped with a scale corresponding to specific gravities from 1,024 to 1,031. the weights consisting of small metal beads.

Usually the observations were performed with the STEEGER-KÜCHLER instruments which had been provided in larger numbers onboard and for which correction tables had been provided. This was not the case for the GREINER instruments. They showed small differences to the former instruments. However, in the case of low values of specific gravity of the water the latter instruments had to be used because the STEEGER ones were not adequate”.

There are several potential sources of error in the specific gravity values reported and analysed here. The most obvious is the multi-stage process between the measurement being made aboard the vessels and recorded in hand-written logs (we are not aware that these still exist) and then to the printed reports and finally to our extraction of values from these reports. We have only been able to eliminate errors in this last step. Other “outliers” in the 1870s data that we have rejected must be attributed to transcription or other unknown errors of observation. The specific gravity measurements are reported to 5 decimal places: a change of 0.00001 in specific gravity $\equiv 0.013 \text{ g kg}^{-1}$ in salinity. i.e. rounding error is ± 0.0065 . Surprisingly there is no discussion in the reports of the possible errors that might be introduced by evaporation from the samples.

Assessing the quality of the 1870s data. The geographical coverage of the Challenger and Gazelle stations at which specific gravity was measured are shown in Fig. 1a which shows the tracks superimposed on the present-day near-surface salinity field from the EN4¹⁰ data set representing conditions from 1950 to 2019 inclusive. In this paper we do not analyse the subsurface values, the distribution of which is shown in Supplementary Information Fig. S1.

Though the Challenger and Gazelle tracks are not ideal for sampling the major features of the global salinity field, they did cross the northern and southern subtropical gyres of the Pacific and Atlantic oceans. Challenger made a single excursion across the Antarctic circumpolar current and Gazelle surveyed the south Indian Ocean. Unfortunately, specific gravity sampling on Gazelle did not start until the vessel had crossed the equator on its outward voyage.

For comparisons between the 1870s surface bucket sampled data and modern values we use the shallowest EN4 level (5 m) and CZ16 (1 m) as being representative of surface values. The post-1990 EN4 data have smaller uncertainties since they include data from the World Ocean Circulation Experiment (1990–1997)^{22,23} and from the Argo profiling float programme²⁴ (2000 onwards and covering the uppermost 2000m)²⁵.

We removed outlying salinity values from the 1870s data based on two passes of a standard deviation filter from the corresponding value in the EN4 reference set. The first pass is three standard deviations, effectively removing egregious data, the second pass is two standard deviations (95% confidence limit). The EN4 and CZ16 reference sets were determined by computing the monthly mean 5 m depth salinity (1 m for CZ16) (1950–1959) for the month of the Challenger or Gazelle observation. The standard deviation of this monthly mean is computed from 10 monthly values from the same month as the Challenger/Gazelle observation.

The first test of the value of the 1870s data is the extent to which they reproduce the present-day variations along ships’ tracks. The comparisons to EN4 are shown in Fig. 4.

From the upper panel it is clear that both the Challenger and Gazelle observations follow the structures in the EN4 data. The close match is seen even for the Challenger excursions into the low salinity region off Nova Scotia (around

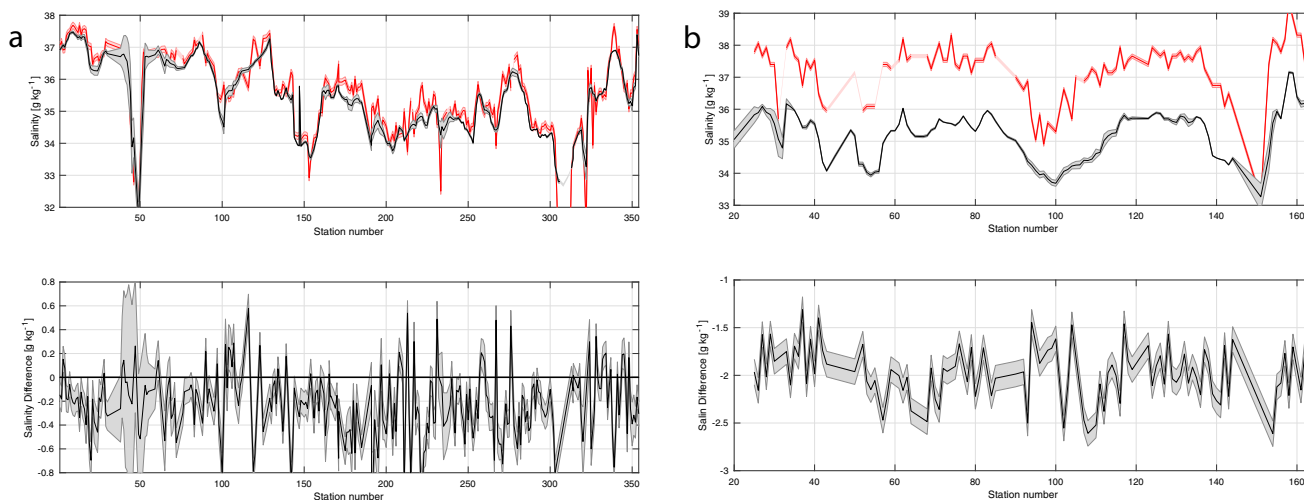


Fig. 4 Along-track comparisons of 1870s salinities with modern-day values. **a** Challenger, **b** Gazelle. Upper panels Black is the 5 m EN4 data (1950–59) and Red are the 1870s observations. Bottom panel is EN4 minus 1870s data. EN4 error bar is ± 1 standard deviation of the monthly mean surface value. Lower panel error bar is the root-sum-square of the errors in the top panel.

Table 2 Global and South Atlantic surface salinity difference and standard deviation and Gazelle duplicate samples.

Data subset	Stns	Mean EN4 _(1950–1959) minus Challenger. g kg^{-1}	Standard deviation	nsamp
Global Challenger	1 to 354	−0.226	0.268	279
Global Gazelle	25 to 164	−1.969	0.289	101
Challenger				
S Atlantic 1873	98–134	−0.120	0.348	26
S Atlantic 1876	322–354	−0.116	0.293	27
Gazelle				
S Atlantic 1874	25–39	−1.808	0.253	13
S Atlantic 1876	151–163	−1.991	0.362	9
Surface duplicates		0.0654	0.2181	70

Region definitions and station numbers in Table S2.

station 50) and into the Southern Ocean (around stations 150 and 310). The *Gazelle* data similarly reproduce the large-scale variations including low salinities at the mouth of the River Congo (Stn 31) and River Plate (Stn 151). We have been unable to identify the cause of the large offset of the *Gazelle* salinities from EN4. However, the central results of the analysis in the main section of this paper, since they are based on the analysis of anomalies, are not affected by the magnitude of the offset.

Aboard *Gazelle*, duplicate samples were taken and sealed in bottles that were returned to Kiel where they were analysed after the voyage. Comparison of the computed salinities of the two data sets shows that they are effectively identical. Differences were $0.065 \pm 0.217 \text{ g kg}^{-1}$ based on 70 duplicate pairs.

The mean difference shows that surface *Challenger* data after the elimination of 15 outliers are saltier than the 1950–1959 EN4 data by $0.224 \pm 0.268 \text{ g kg}^{-1}$ for 276 samples and after the rejection of 9 samples the *Gazelle* are saltier by $1.969 \pm 0.289 \text{ g kg}^{-1}$ for 101 samples.

Consistency of the Challenger and Gazelle data throughout the voyages.

The main analysis in this paper is dependent on there being no large-scale temporal or spatial changes in the Challenger and *Gazelle* sample analysis other than those that might be attributable to changes in evaporation/precipitation. In order to assess the consistency of the determination of specific gravity we took advantage of the fact that both vessels made observations in the South Atlantic during their outward and return voyages (*Challenger* in 1873 and 1876 and *Gazelle* in 1874 and in 1876. We calculated the EN4 minus 1870s offsets and these are summarised in Table 2.

From the fact that for each ship the two visits to the South Atlantic effectively recorded identical salinities (Student's t-test at 90% level), and subject to the proviso that the ship tracks differed in the two occupations, we conclude that the analytical technique used by *Challenger* and *Gazelle* were consistent throughout the voyages and that any regional changes in EN4 minus 1870s data may therefore reflect changes in oceanic conditions.

We also investigated whether there were large ENSO events in the 1870s that might have created significant large-scale perturbations in surface conditions. The classification of ENSO events by Gergis and Fowler²⁶ suggests that there were no such events during the mid 1870s. The longer (1990–2019) EN4 window period did contain several ENSO events but we have assumed that these would have been averaged and so exerted minimal regional bias to EN4.

Data availability

The original specific gravity observations are published in references^{3,21}. The transcribed values have been submitted to the US National Centres for Environmental Information (<https://doi.org/10.25921/jcca-e972>).

Received: 11 November 2020; Accepted: 9 April 2021;

Published online: 26 April 2021

References

- Friedman, A. R., Reverdin, G., Khodri, M. & Gastineau, G. A new record of Atlantic sea surface salinity from 1896 to 2013 reveals the signatures of climate variability and long-term trends. *Geophys. Res. Lett.* **44**, 1866–1876 (2017).
- Thompson, C. W. & Murray, J. Report on the scientific results of the voyage of H.M.S. Challenger during the years 1872–76. <http://www.19thcenturyscience.org/HMSC/HMSC-INDEX/index-linked.htm> (1882–1895).
- Die Forschungsreise, S. M. S. “Gazelle” in den Jahren 1874 bis 1876: unter Kommando des Kapitän See Freiherrn von Schleinitz, Vol. 2–5 (E. S. Mittler und Sohn, 1889–90).

4. Hawkins, E. et al. Estimating changes in global temperature since the preindustrial period. *Bull. Amer. Meteor. Soc.* **98**, 1841–1856 (2017).
5. McDougall, T. J., Jackett, D. R., Millero, F. J., Pawlowicz, R. & Barker, P. M. A global algorithm for estimating absolute salinity. *Ocean Sci.* **8**, 1123–1134 (2012).
6. Durack, P. J. & Wijffels, S. E. Fifty-year trends in global ocean salinities and their relationship to broad-scale warming. *J. Clim.* **23**, 4342–4362 (2010).
7. Durack, P. J., Wijffels, S. E. & Boyer, T. P. in *Ocean Circulation and Climate: A 21st Century Perspective*, Vol. 103 (eds Siedler, G., Griffies, S. M., Gould, J. & Church, J. A.) 727–757 (Academic, Elsevier, 2013).
8. Durack, P. J., Wijffels, S. E. & Matear, R. J. Ocean salinities reveal a strong global water cycle intensification during 1950–2000. *Science* **336**, 455 (2012).
9. Cheng, L. et al. Improved estimates of changes in upper ocean salinity and the hydrological cycle. *J. Climate* **33**, 10357–10381 (2020).
10. Good, S. A., Martin, M. J. & Rayner, N. A. EN4: quality controlled ocean temperature and salinity profiles and monthly objective analyses with uncertainty estimates. *J. Geophys. Res. Oceans* **118**, 6704–6716 (2013).
11. Taylor, K. E., Stouffer, R. J. & Meehl, G. A. An overview of CMIP5 and the experiment design. *Bull. Amer. Meteor. Soc.* **93**, 485–498 (2012).
12. Morice, C. P. et al. An updated assessment of near-surface temperature change from 1850: the HadCRUT5 dataset. *J. Geophys. Res.* **126**, e2019JD032361 (2020).
13. Kennedy, J. J., Rayner, N. A., Atkinson, C. P. & Killick, R. E. An ensemble data set of sea surface temperature change from 1850: the Met Office Hadley Centre HadSST.4.0.0.0 data set. *J. Geophys. Res. Atmos.* **124**, 7719–7763 (2019).
14. Zika, J. D. et al. Improved estimates of water cycle change from ocean salinity: the key role of ocean warming. *Environ. Res. Lett.* **13**, 0740367 (2018).
15. Hubble, E. A relation between distance and radial velocity among extragalactic nebulae. *Proc. Natl Acad. Sci. USA* **15**, 168–173 (1929).
16. Dittmar, W. Report on researches into the composition of ocean water collected by H.M.S. Challenger. *Challenger Rep. Phys. Chem* **1**, 1–251 (1884).
17. Forch, C., Knudsen, M. & Sørensen, S. P. L. "Berichte über die Konstantenbestimmungen zur Aufstellung der hydrographischen Tabellen. D. Kgl. Danske Vidensk. Selsk. Skrifter, 6". *Raekke Naturvidensk. Og Mathem. Afd. XII* **1**, 151 (1902).
18. Buchanan, J. Y. On the determination, at sea, of the specific gravity of seawater. *Proc. R. Soc. London* **23**, 301–308 (1875).
19. Buchanan, J. Y. The Hydrometer as an instrument of precision. *Nature* **91**, 229–230 (1913).
20. Buchanan, J. Y. Experimental researches on the specific gravity and the displacement of some saline solutions. *P. Roy. Soc. Edin.* **49**, 1–227 (1914).
21. Thompson, C. W. & Murray, J. Report on the scientific results of the voyage of H.M.S. Challenger during the years 1872–76. Summary of scientific results, first part. <https://www.biodiversitylibrary.org/bibliography/6513#summary> (1895).
22. Sparrow, M., Chapman, P. & Gould, J. (eds.) *The World Ocean Circulation Experiment (WOCE) Hydrographic Atlas Series* Southampton, UK. International WOCE Project Office. <http://woceatlas.ucsd.edu/> (2005).
23. WOCE. *World Ocean Circulation Experiment, Global Data, Version 3.0*. WOCE International Project Office, WOCE Report, Southampton, UK (U.S. National Oceanographic Data Center, 2002).
24. Riser, S. et al. Fifteen years of ocean observations with the global Argo array. *Nat. Clim. Change* **6**, 145–153 (2016).
25. Wong, A. P. S. et al. Argo data 1999–2019: two million temperature-salinity profiles and subsurface velocity observations from a global array of profiling floats. *Front. Mar. Sci.* **7**, 700 (2020).

26. Gergis, J. L. & Fowler, A. M. A history of ENSO events since A.D. 1525: implications for future climate change. *Clim. Change.* **92**, 343 (2009).

Acknowledgements

We are grateful for the translations of the Gazelle reports by Prof. G. Siedler and for the comments by the reviewers. S.A.C. was supported by UK NERC National Capability programmes the Extended Ellett Line and CLASS (NE/R015953/1), NERC grants UK OSNAP (NE/K010875/1, NE/K010875/2, NE/K010700/1), UK OSNAP Decade (NE/T00858X/1, NE/T008938/1), the Blue-Action project (European Union's Horizon 2020 research and innovation programme, grant 727852) and the iAtlantic project (European Union's Horizon 2020 research and innovation programme, grant 210522255). HadCRUT5.0.1.0 surface air temperatures were obtained from <https://www.metoffice.gov.uk/hadobs/hadcrut5/data/current/download.html> on 25th March 2021 and HadSST.4.0.0.0 sea-surface temperatures from <https://www.metoffice.gov.uk/hadobs/hadsst4/> on 25th March 2021 and are ©British Crown Copyright, Met Office provided under an Open Government License v3 <http://www.nationalarchives.gov.uk/doc/open-government-licence/version/3/>. The Cheng et al. data set was obtained from <http://159.226.119.60/cheng/> on 4th January 2021.

Author contributions

W.J.G. conceived the study and transcribed the *Challenger* and *Gazelle* information from the original printed reports. S.A.C. carried out all computations and statistical analysis. The interpretation and manuscript preparation were carried out jointly.

Competing interests

The authors declare no competing interests.

Additional information

Supplementary information The online version contains supplementary material available at <https://doi.org/10.1038/s43247-021-00161-3>.

Correspondence and requests for materials should be addressed to W.J.G.

Peer review information Primary handling editors: Regina Rodrigues, Heike Langenberg

Reprints and permission information is available at <http://www.nature.com/reprints>

Publisher's note Springer Nature remains neutral with regard to jurisdictional claims in published maps and institutional affiliations.



Open Access This article is licensed under a Creative Commons Attribution 4.0 International License, which permits use, sharing, adaptation, distribution and reproduction in any medium or format, as long as you give appropriate credit to the original author(s) and the source, provide a link to the Creative Commons license, and indicate if changes were made. The images or other third party material in this article are included in the article's Creative Commons license, unless indicated otherwise in a credit line to the material. If material is not included in the article's Creative Commons license and your intended use is not permitted by statutory regulation or exceeds the permitted use, you will need to obtain permission directly from the copyright holder. To view a copy of this license, visit <http://creativecommons.org/licenses/by/4.0/>.

© The Author(s) 2021